Estuaries Vol. 17, No. 1B, p. 187–199 March 1994

Refining Habitat Requirements of Submersed Aquatic Vegetation: Role of Optical Models

CHARLES L. GALLEGOS
Smithsonian Environmental Research Center
P.O. Box 28
Edgewater, Maryland 21037

ABSTRACT: A model of the spectral diffuse attenuation coefficient of downwelling irradiance was constructed for Chincoteague Bay, Maryland, and the Rhode River, Maryland. The model is written in terms of absorption spectra of dissolved yellow substance, the chlorophyll-specific absorption of phytoplankton, and absorption and scattering by particulate matter (expressed as turbidity). Based on published light requirements for submersed aquatic vegetation (SAV) in Chesapeake Bay, the model is used to calculate the range of water-quality conditions that permit survival of SAV at various depths. Because the model is spectrally based, it can be used to calculate the attenuation of either photosynthetically active radiation (PAR, equally weighted quanta from 400 nm to 700 nm) or photosynthetically *usable* radiation (PUR, the integral of the quantum spectrum weighted by the pigment absorption spectrum of SAV). PUR is a more accurate measurement of light that can be absorbed by SAV and it is more strongly affected by phytoplankton chlorophyll in the water column than is PAR. For estuaries in which light attenuation is dominated by turbidity and chlorophyll, the model delimits regions in which turbidity alone (chlorophyll < 10 μg l^{-1}), chlorophyll alone (turbidity < 1 NTU) or both factors (chlorophyll > 10 μg l^{-1}, turbidity > 1 NTU) must be reduced to improve survival depths for SAV.

Introduction

Coastal seagrass habitats are highly valued for their contribution to primary productivity, as a refuge for larval and juvenile fish, and for trapping of suspended sediments and stabilization of bottom sediments. Consequently, loss of seagrass habitat is one of the major threats to the environmental quality in many estuaries (Thayer et al. 1975; Orth and Moore 1983).

The causes of seagrass decline may vary from site to site. Commonly cited factors include disease (Short et al. 1988), herbicides (Correll and Wu 1982), excessive growth of epiphytes caused by allocthonous nutrient loading (Twilley et al. 1985), and reduction of water-column transparency (Dennison 1987; Giesen et al. 1990). The latter two factors directly affect the light available at the surface of the plant leaf. Recent studies (Duarte 1991) indicate that, while light requirements differ among species, seagrasses in general have among the highest light requirements (expressed as a percentage of full sunlight) in the plant kingdom (reviewed by Dennison et al. 1993). *Zostera marina,* for example, requires about 20% of surface-incident irradiance for survival (Dennison 1987; Dennison et al. 1993). Furthermore, controlled experiments in mesocosms subjected to varying degrees of shading indicated that growth of *Z. marina* continued to respond positively to increases in irradiance up to full sunlight (Short 1991).

It is clear that maintaining adequate light penetration to the depth limit of an existing seagrass bed is a minimal requirement for preservation of the bed. Similar constraints apply to the choice of a site for attempted restoration by planting. It is important, therefore, to know what concentrations of optically-important constituents will permit maintenance and growth of seagrasses at a given site.

Dennison et al. (1993) recently synthesized results of a multiannual study of submersed aquatic vegetation (SAV) distributions in relation to water quality in Chesapeake Bay. Using correspondence analysis, they found that sites with persistent or fluctuating seagrass beds to depths of 1 m or greater occurred only where median concentrations of total suspended solids (TSS) and chlorophyll concentrations were <15 mg l^{-1} and <15 μg l^{-1} respectively during the growing season, and, simultaneously, median K_d(PAR) was <1.5 m^{-1}. Their approach, which does not require a detailed understanding of the relationship between water quality and light attenuation, has the advantage that it uses the plants themselves as an "integrating light meter" to assess light regimes and associated water quality on temporal scales appropriate to SAV survival. A limitation of the approach is that only the combinations of median water-quality concentrations actually observed at the sites examined can be evaluated for their suitability. For example, only one site in their Fig. 5a fell within the region in the parameter-space defined by (TSS < 15 mg l^{-1}) ∩ (chlorophyll > 15 μg l^{-1}). Additionally, habitat requirements for factors (e.g., dissolved organ-

0160-8347/94/01B0187-13$01.50/0

ic matter) that are not presently dominant contributors to attenuation in Chesapeake Bay, but are important elsewhere (McPherson and Miller 1987), cannot be established. Thus, correspondence analysis is site-specific.

The studies that defined the light requirements for seagrasses were generally based on Secchi disk transparencies or on calculations of the diffuse attenuation coefficient for photosynthetically active radiation (PAR, 400–700 nm) measured using quantum sensors with wide spectral sensitivity (Duarte 1991). While PAR adequately quantifies the light available for plant photosynthesis, it is inadequate for developing a general model of the factors causing the attenuation. Regressions of the diffuse attenuation coefficient for downwelling PAR, K_d(PAR), against water-quality constituents are valid only over the range of concentrations observed. Frequently one factor such as suspended solids (Vant 1990) or color (McPherson and Miller 1987) dominates attenuation. Because scattering and absorption combine nonlinearly to produce attenuation (see below), regression equations developed from one set of conditions cannot, in general, be used to predict the response to increases in another variable beyond levels encountered. Furthermore, concentrations of attenuation-producing substances may covary, so that regressions of K_d(PAR) against water-quality measurements tend to be site-specific and lack power to resolve the effects of different components.

Instruments that measure PAR (in principle) weight all quanta equally in the wavelength range from 400 nm to 700 nm. Quanta at all wavelengths are not, however, absorbed with equal efficiency by plant photosynthetic pigments. Similarly, the factors that contribute to light attenuation in estuaries exhibit characteristic spectral selectivity (see below), so that the spectrum of available light changes with depth in a way that depends on the particular combination of water-quality constituents present. Morel (1978) defined the concept of photosynthetically *usable* radiation (PUR) as the integral of the quantum spectrum (400–700 nm) weighted by the relative absorption spectrum of the plants of interest. Two different combinations of water-quality parameters may produce identical values of photon flux density (PAR) but different values of PUR if the spectrum of available photons produced by one combination is better matched to the plant absorption spectrum than the other.

The distinction between PAR and PUR is potentially important for determining habitat requirements for submersed aquatic vegetation. For example, phytoplankton, being photosynthetic organisms, absorb light at a spectral selectivity similar to higher rooted plants; we might expect, therefore, that the attenuation of PUR would be more sensitive to phytoplankton chlorophyll than that of PAR. Chambers and Prepas (1988) hypothesized that macrophyte depth limits in lakes in Alberta, Canada, were shallower in humic-stained lakes compared with oligotrophic lakes, due to the selective absorption of blue wavelengths by humic substances. To make the distinction between PAR and PUR, it is necessary to measure the spectrum of available irradiance or to calculate it from a suitably calibrated model of the dependence of spectral attenuation on water-quality parameters.

I present a procedure for determining water-quality concentrations that meet specified penetration requirements for different depth intervals. The procedure uses the equation of Kirk (1984) for K_d in terms of absorption and scattering coefficients to calculate the propagation of spectral irradiance underwater; the spectra may be integrated with or without weighting to calculate PAR or PUR. Absorption coefficients are calculated from laboratory measurements of spectrally-variable specific-absorption coefficients of optically-important water-quality components; the scattering coefficient is estimated from turbidity (Vant 1990). Field studies and optical measurements of water-quality parameters were made in the Rhode River, Maryland, a site where SAV disappeared in the early 1970s, and in Chincoteague Bay, Maryland, over and adjacent to an accreting bed of *Zostera marina*.

Model Development

The empirical descriptor of the light available at a depth in terms of that available at the surface is the diffuse attenuation coefficient of downward propagating irradiance, K_d, defined as

$$K_d = -\frac{1}{z}\ln\left(\frac{E_z}{E_{0^-}}\right) \quad (1)$$

where E_z is the irradiance available at depth z, and E_{0^-} is the irradiance just below the surface (0^-) (Morel and Smith 1982). The definition is useful because the decrease in irradiance with depth is *approximately* exponential. The depth to which, say, 20% of surface-incident irradiance penetrates, Z_{20}, is easily determined from Eq. (1) as

$$Z_{20} = \frac{-\ln(0.20)}{K_d} = \frac{1.61}{K_d} \quad (2)$$

where the negative sign converts depth to positive distance below the water surface.

The diffuse attenuation coefficient is referred to as an apparent optical property (Kirk 1981) because its value depends on the ambient underwater light field. Its magnitude changes as the angular distribution of the underwater light field changes

with depth or with cloud cover, and it depends on the sun as a light source. Because of the dependence on the ambient light field, K_d cannot, in principle, be decomposed into contributions due to separate components, although it is sometimes attempted as an approximation (Smith 1982).

Properties that do not depend on the ambient light field either for their definition or for their measurement are called inherent optical properties (Kirk 1981). Inherent optical properties, in particular the total absorption coefficient, α_t, and the scattering coefficient, b, have the property that the contributions due to different materials are additive, and the partial contribution due to each material is linear with its concentration. The proportionality constant between, for example, absorption coefficient and the concentration of a constituent is called the specific absorption coefficient of the material.

The relationship between K_d and inherent optical properties is the subject of continuing research (Kirk 1991; Gordon 1991), principally by Monte Carlo simulation of the equations of radiative transfer. A useful relationship is one determined by Kirk (1984)

$$K_d = \frac{1}{\mu_0}[a_t^2 + G(\mu_0)\, a_t b]^{1/2} \tag{3}$$

where μ_0 = cosine of the zenith angle of the direct solar beam refracted at the air-water interface (a function of latitude, date, and time of day), and $G(\mu_0)$ is a function

$$G(\mu_0) = g_1\mu_0 - g_2 \tag{4}$$

that modifies the interaction between scattering and absorption; and g_1 and g_2 are coefficients that depend on the scattering phase function (an inherent optical property) of the water column and on the optical depth of interest (Kirk 1991). Values of g_1 and g_2 have been determined for depth intervals from the surface down to the 1% penetration depth and for a small depth increment about the 10% penetration depth, both for waters having volume scattering functions typical of turbid coastal water (Kirk 1984). Unfortunately, g_1 and g_2 have not been determined for the depth interval from the surface down to Z_{20}, the approximate depth at which SAV can survive. In the ensuing analysis, I used the coefficients determined for the surface to the 1% penetration depth.

To predict K_d from water-quality measurements, a_t and b must be specified in terms of optically-important water-quality concentrations. As indicated above, a_t may be expressed as the sum

$$a_t = a_y + a_{ph} + a_d + a_w \tag{5}$$

where the subscripts indicate contributions due to dissolved yellow substance (y), phytoplankton (ph), particulates other than phytoplankton (d), and water itself (w). In estuaries, scattering due to particles far exceeds that due to water itself, so that b need not be decomposed into components.

In general, both a_t and b may depend on wavelength, λ. Although some studies have found b to be independent of wavelength (Witte et al. 1982; Phillips and Kirk 1984), I used the $1/\lambda$ dependence of Morel and Gentili (1991), with $b(550)$ = [Turb] (see, e.g., Weidemann and Bannister 1986; Vant 1990). Thus, I represented scattering by the equation

$$b(\lambda) = \left(\frac{550}{\lambda}\right)[\text{Turb}]. \tag{6}$$

The wavelength dependence of a_y in the visible region of the spectrum may be expressed simply as a negative exponential (Bricaud et al. 1981)

$$a_y(\lambda) = g_{440}\exp[-s_y(\lambda - 440)] \tag{7}$$

where g_{440} = absorption by dissolved yellow matter (*gelbstoff*) at 440 nm, and $s_y = 0.014\ \text{nm}^{-1}$ for most coastal waters (Bricaud et al. 1981); g_{440} was recently proposed as a measure of water color (Cuthbert and del Giorgio 1992) and correlates well with color as conventionally measured in Pt units (Bowling et al. 1986).

Typically measurements of a_d, absorption by mineral and nonalgal organic particulate matter, decrease exponentially in the visible domain to some asymptote in the longwave ($\lambda > 700$) region of the spectrum (see below, Fig. 1). Previous authors (Roessler et al. 1989; Gallegos et al. 1990) have subtracted the longwave asymptote and used expressions similar to Eq. 7 to model a_d. This procedure attributes all in situ absorption at $\lambda > 700$ nm to water alone. Previously, Gallegos et al. (1990) estimated b from measurements of $K_d(720)$ by rearranging Eq. 3 and assuming $a_t(720) \approx a_w(720)$. Here I found that attributing all absorption in the 720 nm waveband to water alone produced estimated scattering coefficients that seemed too high. In one case b estimated by the old procedure was $>100\ \text{m}^{-1}$, and estimates were always well in excess of measured turbidity, which has been found by other authors to correlate well with b with a proportionality constant of very nearly 1 (Weidemann and Bannister 1986; Vant 1990). The variable longwave asymptote in the measurements of a_d correlated well with both suspended solids and with turbidity (see below, Results). When longwave absorption by nonalgal particulate matter was added to $a_w(720)$ the resulting estimates of b were compatible with Eq. 6 (see also Maske and Haardt 1987). Thus I modeled absorption by nonalgal particulate matter as

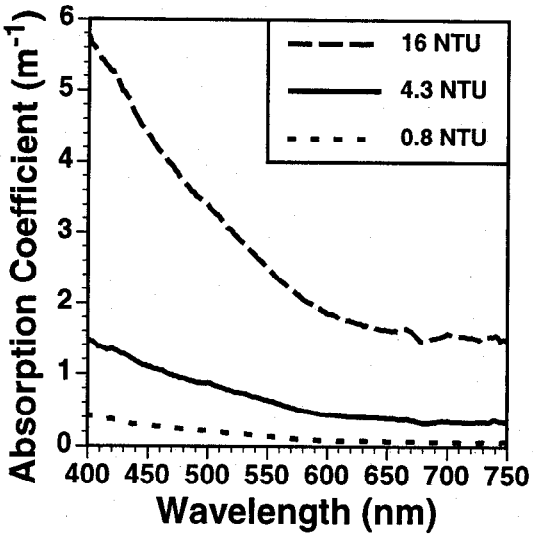

Fig. 1. Absorption by particulate matter collected on glass fiber filter and extracted in methanol to remove soluble phytoplankton pigments. Samples are from Chincoteague Bay and span the range of observed turbidity (NTU). Baseline at long wavelengths has not been subtracted.

$$a_d(\lambda) = \sigma_d(\lambda)[\text{Turb}] \quad (8a)$$

and

$$\sigma_d(\lambda) = \sigma_{bl} + \sigma_{400}\exp[-s_d(\lambda - 400)] \quad (8b)$$

where [Turb] = turbidity (NTU), σ_d is the specific absorption coefficient of turbidity, σ_{bl} is the long-wave specific absorption coefficient, σ_{400} scales the absorption amplitude at short wavelengths, and s_d determines the rate of exponential decrease to σ_{bl}. I used [Turb] in preference to [TSS] because of its ease of measurement, superior analytical precision, and use in many water-quality monitoring programs.

The wavelength dependence of a_{ph} does not have a convenient functional form but must be expressed in terms of the chlorophyll concentration, [Chl], and wavelength-dependent chlorophyll-specific absorption, $a^*_{ph}(\lambda)$,

$$a_{ph}(\lambda) = a^*_{ph}(\lambda)[\text{Chl}] \quad (9)$$

$a^*_{ph}(\lambda)$ may be measured, as in this work, or taken from tabulated values in the literature (e.g., Prieur and Sathyendranath 1981). Absorption by water is taken from tabulated values of $a_w(\lambda)$ (Smith and Baker 1981).

Equations 6–9 substituted into Eq. 5 and Eq. 3 express the dependence of spectral diffuse attenuation coefficient on water-quality variables. To calculate the penetration of PAR either from the model or from measured $K_d(\lambda)$, the spectrum of incident sunlight, E_{0^-} (Weast 1980), converted to units of quantum flux density, is propagated in 5-nm wavebands to a reference depth, z_r, according to

$$E_{z_r}(\lambda) = E_{0^-}(\lambda)\exp[-K_d(\lambda)z_r]. \quad (10)$$

At z_r, $\widehat{PAR}_z$ is calculated by numerical integration of $E_{z_r}(\lambda)$ from λ = 400 nm to 700 nm. The spectrally-estimated diffuse attenuation for PAR, $K_d(\widehat{PAR})$ is calculated as

$$K_d(\widehat{PAR}) = \frac{1}{z_r}\ln\left(\frac{\widehat{PAR}_z}{PAR_0}\right) \quad (11)$$

where the carat distinguishes spectral estimates from field measurements made with broadband sensors. Z_{20} for PAR is calculated from $K_d(\widehat{PAR})$ by Eq. 2. Habitat requirements are determined by varying the water-quality concentrations of [g_{440}], [Turb], and [Chl] over suitable ranges, and determining combinations of variables producing predictions of $Z_{20} \geq$ various target depths. The diffuse attenuation for PUR was calculated in a similar manner as Eq. 11 except that the quantum spectra at the surface and at z_r were weighted by a relative absorption spectrum measured for *Z. marina*.

Calibration and Data Requirements

To implement the model of spectral diffuse attenuation coefficient, the specific-absorption coefficients σ_{bl} and σ_{400}, the spectral slope, s_d, of turbidity, and tabulations of the chlorophyll-specific absorption spectrum, $a^*_{ph}(\lambda)$, are needed. Roessler et al. (1989) summarized mean values of s_y (0.014 nm^{-1}), which is the value I used here. The water-quality data required to predict the spectrum of diffuse attenuation coefficients according to this model are [Turb], from which b and $a_d(\lambda)$ are predicted using Eqs. 6 and 8b respectively, [Chl] for estimation of $a_{ph}(\lambda)$ (Eq. 9), and color as g_{440} for estimation of $a_y(\lambda)$ (Eq. 7). μ_0 is calculated from location, date, and time of day (Smithsonian Meteorological Tables) and used with Eq. 3 to predict $K_d(\lambda)$.

Materials and Methods

Study Sites

In situ measurements were carried out between June 1991 and December 1992 in the Rhode River, Maryland (38°52′N, 76°32′W) (Gallegos et al. 1990), and in Chincoteague Bay, a shallow bar-built estuary on the Maryland-Virginia border (37°59′N, 75°22′W). At Chincoteague Bay, sites were occupied roughly along a west-east transect across the middle two-thirds of the bay beginning at Greenbackville, Maryland. Depths at the stations occupied ranged from 0.5 m to 3.25 m. Salinity varied only slightly, from 30‰ to 34‰. The sea-

grass beds occur on a shallow bar along the east side of the bay.

The Rhode River is a shallow, eutrophic subestuary on the western shore and in the mesohaline reach of Chesapeake Bay. Measurements were made off the dock at the Smithsonian Environmental Research Center, using a boom that extended 2 m off the sunward side of the pier. The spectrum of downwelling diffuse attenuation was previously described for the Rhode River by Pierce et al. (1986) and Gallegos et al. (1990).

Field Measurements

Profiles of downwelling, cosine-corrected, spectral irradiance were measured using the submersible radiometer described by Gallegos et al. (1990). Wavebands of the spectrum are isolated using interference filters (Corion Corporation) that vary in bandwidths; narrowest bandwidths are used in the region of the spectrum in which diffuse attenuation coefficients change most rapidly. Details of spectral response of the instrument are given by Gallegos et al. (1990), except that a 40-nm bandwidth filter centered at 550 nm was used instead of one of the 500-nm filters inadvertently duplicated in that work. During part of this study, profiles of quantum scalar irradiance (4π, 400–700 nm) were measured with a Biospherical Instruments QSP-200 probe and QSP-170B readout.

Voltages for each channel of the spectral radiometer were normalized to readings from a deck cell; percentage of surface irradiance reaching each depth was calculated by dividing the normalized readings by the normalized reading at the surface taken at the start of a profile. Diffuse attenuation coefficients were calculated from the slope of a regression of log-transformed percentages against depth (Gallegos et al. 1990). Diffuse attenuation coefficient for quantum scalar irradiance, K_0(PAR) was calculated in a similar manner, except that profiles were kept brief so that normalization to surface incident readings was not needed.

Laboratory Analyses

Vertically integrated water samples were collected with a 2-l Labline Teflon water sampler by lowering and raising the bottle at a constant rate in less time than required to completely fill the bottle. Samples were placed on ice in a cooler and returned to the laboratory for analysis. Water samples were analyzed for total and mineral suspended solids, Chl *a*, and absorption by dissolved and particulate matter by methods described previously (Gallegos et al. 1990). Turbidity was measured with a Hach model 2100A turbidimeter calibrated against formazin standards (Cole Parmer). Samples from Chincoteague Bay were filtered for Chl *a* and particulate absorption analyses immediately upon return to the laboratory (within ca. 8 h); samples for suspended solids analyses and absorption by dissolved matter were filtered the day after collection. Samples from the Rhode River were filtered for all analyses in <2 h.

Results

Calibration of Optical Model

Absorption by mineral and nonalgal organic particulates exhibited an exponential decrease with wavelength to a longwave asymptote that depended on [Turb] (Fig. 1). Absorption by nonalgal particulates in each of the wavebands covered by the spectral radiometer was linearly related to [Turb] (Fig. 2a); for clarity only three wavebands are shown. Slope of the regression of $a_d(\lambda)$ against [Turb] was highest in the short wavelength end of the visible spectrum and decreased to a constant baseline in a manner well described by Eq. 8b (Fig. 2b). Coefficients of determination of the individual linear regressions ranged from 0.82 (720 nm) to 0.90 (650 nm) and were generally about 0.88. Estimated parameters in Eq. 8b were $\sigma_{bl} = 0.116$ m^{-1} NTU^{-1}, $\sigma_{400} = 0.258$ m^{-1} NTU^{-1}, $s_d = 0.0165$ nm^{-1}.

Chlorophyll-specific absorption by phytoplankton (Fig. 3) was higher in this study than that estimated previously by Gallegos et al. (1990). Variability of $a^*_{ph}(\lambda)$ was high; the coefficient of variation at the 436-nm peak was 24%.

Model Evaluation

Comparison With Spectral Measurements

Results of predictions for Chincoteague Bay and the Rhode River are given in Figs. 4 and 5, respectively. Predictions of $K_d(\lambda)$ were unbiased over a range of observed values from 0.4 m^{-1} to 10 m^{-1} (Figs. 4a and 5a). Average percent deviations (100|observed − predicted|/observed) for the three wavebands in Figs. 4a and 5a were 16.2% and 13.4% respectively. The overall shape of the diffuse attenuation spectra were well modeled in both turbidity-dominated Chincoteague Bay (Fig. 4b) and in the phytoplankton-dominated Rhode River (Fig. 5b).

Comparison With Broadband Measurements

Estimates of $K_d(\widehat{PAR})$ made from measured $K_d(\lambda)$ were highly correlated with measurements of K_0(PAR) (Fig. 6a, squares) but tended to overestimate K_0(PAR) at higher values. Attenuation coefficients measured in the 600 nm waveband of the spectral radiometer, $K_d(600)$, were also highly correlated with K_0(PAR) and were closer to being an

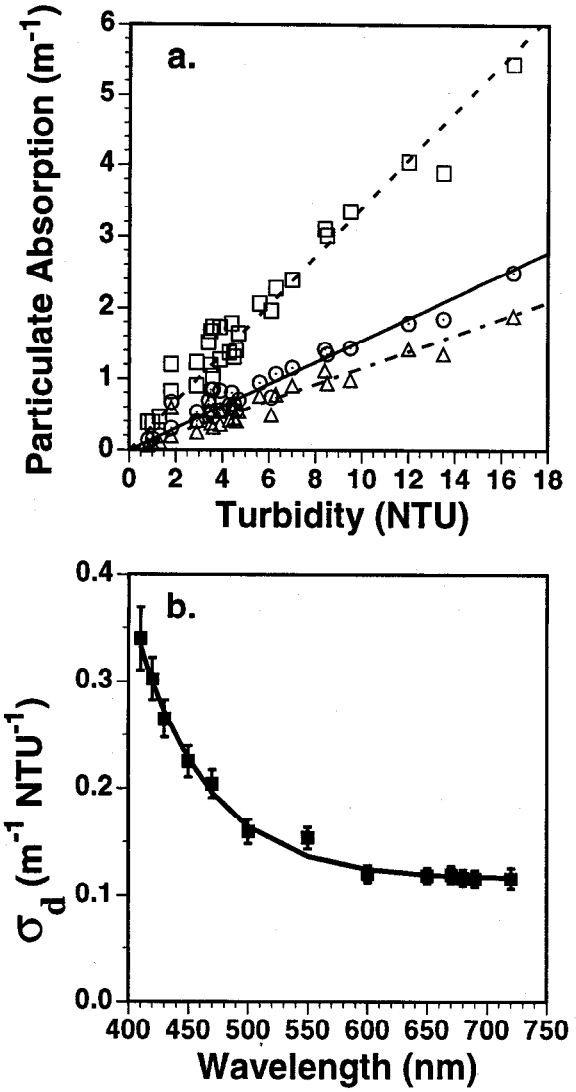

Fig. 2. Absorption by non-algal particulate matter in Chincoteague Bay, Maryland. a. Absorption coefficient at: -----□----- 410 nm; ——⊙—— 550 nm; and –·–·–△–·–·– 720 nm as a function of measured turbidity. b. Slopes of regressions of particulate absorption against turbidity as a function of wavelength. Error bars are 1 SE of regression slopes. Fitted curve is Eq. 8b.

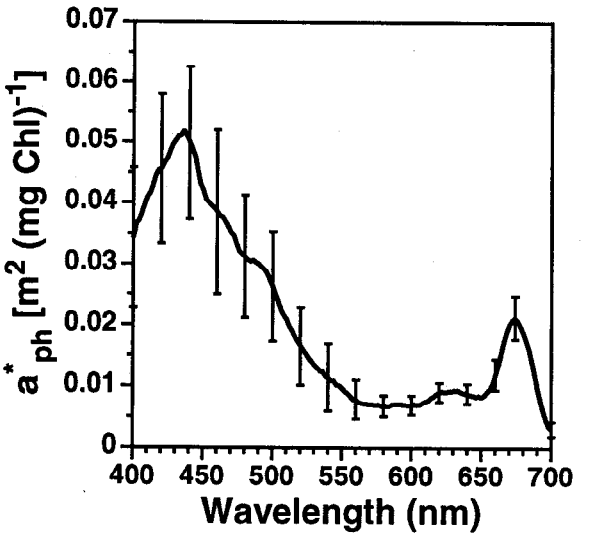

Fig. 3. Chlorophyll-specific absorption by phytoplankton from the Rhode River, Maryland in 15 randomly selected samples having chlorophyll concentration > 30 μg l^{-1}. Error bars are ±1 SD.

unbiased estimator (Fig. 6a, circles). Predictions of the optical model averaged over 585–620 nm (the bandpass of the 600-nm filter in the spectral radiometer) agreed well with measurements of K_0(PAR) (Fig. 6b); coefficient of determination was 0.82 and standard deviation of predictions of K_0(PAR) was 0.25 m^{-1}. In applying the water-quality optical model to estimate habitat requirements, I used the average over this waveband as the estimate of diffuse attenuation coefficient for PAR most likely to correlate with broadband sensors used in most field studies.

Sources of Uncertainty

Sources of error in predictions of diffuse attenuation coefficient were examined by a Monte Carlo procedure that simulated random errors in model coefficients and in water-quality parameters separately and combined. The model coefficients s_y, σ_{bb}, σ_{400}, and s_d were error-corrupted by adding a random normal deviate with mean = 0 and standard deviation = 15% of the calibrated value. Chlorophyll-specific absorption by phytoplankton, $a^*_{ph}(\lambda)$, and wavelength-dependent scattering (Eq. 6) were error-corrupted by multiplying the functions at all wavelengths by a scalar with a mean of 1 and standard deviation of 0.15. Water-quality parameters were corrupted in a similar manner as model coefficients (i.e., by adding a random normal deviate with mean = 0 and standard deviation = 15% of the assumed value to simulate the combined error due to analytical precision and sample repeatability). Mean water-quality values were g_{440} = 0.3 m^{-1}, [Chl] = 15 μg l^{-1}, and [Turb] = 5 NTU; predicted diffuse attenuations for the calibrated model assuming correct coefficients for the assumed water-quality measurements are K_d(600) = 1.52 m^{-1} and K_d(PUR) = 2.04 m^{-1}.

Predictions of diffuse attenuation coefficients for the 600 nm waveband and for PUR, with errors in coefficients and input variables as assumed, were generally normal and unbiased with respect to predictions without errors (Table 1). Coefficients of variation were about 7–8% for errors due to variations in model coefficients, 9–11% for errors in water-quality variables, and 11–13% for combined

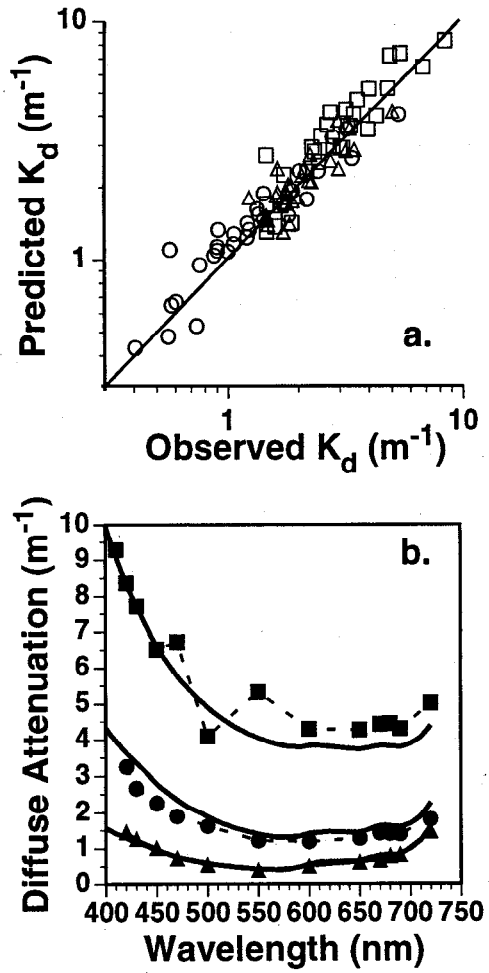

Fig. 4. Evaluation of model predictions against data from Chincoteague Bay. a. Predicted and observed spectral diffuse attenuation coefficients for (□) 420 nm, (○) 550 nm, and (△) 720 nm. Line represents 1:1 correspondence. b. Evaluation of spectra of diffuse attenuation coefficient predicted by the model for (■) the most turbid, (▲) the least turbid, and (●) average spectra for Chincoteague Bay. Bold lines are model predictions.

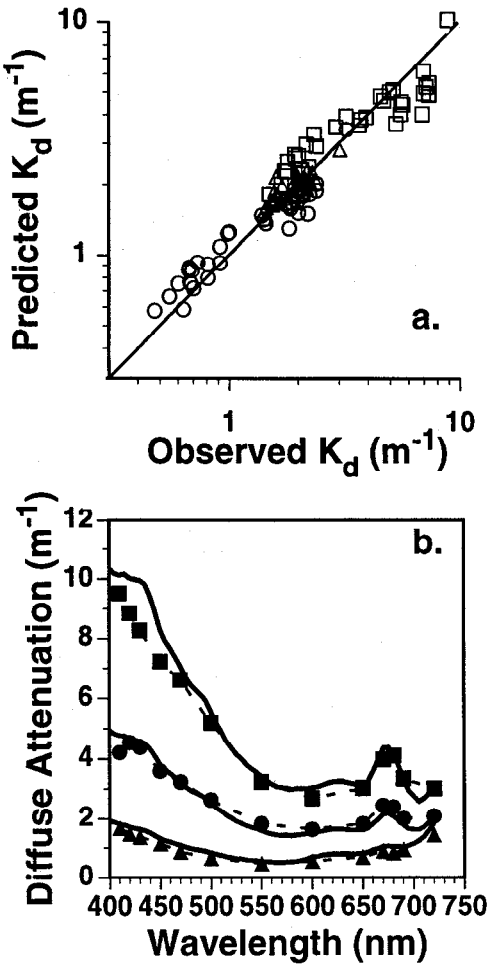

Fig. 5. Evaluation of model predictions against data from Rhode River. a. Predicted and observed spectral diffuse attenuation coefficients for (□) 420 nm, (○) 550 nm, and (△) 720 nm. Line represents 1:1 correspondence. b. Evaluation of spectra of diffuse attenuation coefficient predicted by the model for (■) the most turbid, (▲) the least turbid, and (●) average spectra for the Rhode River. Bold lines are model predictions.

errors. Similar results were obtained with water-quality conditions simulating chlorophyll-dominated attenuation (i.e., $g_{440} = 0.5\ m^{-1}$, [Chl] = 60 μg l^{-1}, [Turb] = 1.5 NTU), and for $K_d(\widehat{PAR})$ (data not shown). Coefficients of variation of simulations were less than those assumed in the coefficients and inputs, probably because of the negative exponential wavelength dependence of absorption by turbidity and *gelbstoff*, and the dominance of absorption in the red by water itself (assumed to be error-free). The standard deviations in columns 6 and 7 of Table 1 are similar to the standard deviation of predictions in Fig. 6b (0.25 m^{-1}), indicating that the degree of correspondence of model predictions with observations is about as expected for the degree of uncertainty assumed here.

Model Application

Augmenting the Data

One useful application of the optical water-quality model is to determine the suitability for SAV survival of water-quality conditions not encountered in measured data. This was done by a Monte Carlo approach in which water-quality concentrations were drawn from random distributions and were input to the optical model to calculate spectral and PAR diffuse attenuation coefficients. Prior to investigating conditions not encountered, the model was checked to see if it would reproduce relationships between diffuse attenuation coefficients and water quality within the range of conditions actually encountered at the sites examined (Figs. 7 and 8). Statistical characteristics of the wa-

ter-quality parameters used in the Monte Carlo simulations are given in Table 2. In the Monte Carlo simulation, correlations between water-quality parameters were set at their sample estimates regardless of statistical significance, because the intent of the analysis was to simulate data similar to that observed, rather than to draw inferences about the water quality data itself.

Plots of both simulated and observed $K_d(600)$ [the best predictor of $K_0(PAR)$] against [Turb] (Figs. 7a and 8a) revealed that light penetration in both Chincoteague Bay and Rhode River is strongly governed by turbidity. Relationships of $K_d(600)$ to [Chl] exhibited much greater scatter (Figs. 7b and 8b); at Chincoteague Bay the range of observed [Chl] was too narrow to permit estimation of a reliable regression between $K_d(600)$ and [Chl] (Fig. 7b). At the eutrophic Rhode River greater influence by [Chl] was observed (Fig. 8b). Except for the higher correlation between $K_d(600)$ and [Turb] in the simulated data for Chincoteague Bay (r^2 = 0.99 and 0.92 for simulated and observed, respectively), similar regressions and degree of scatter were produced by Monte Carlo application of the model as was observed in the data. The higher scatter in measured data from Chincoteague Bay (as compared with the simulation, Fig. 7a) may be a result of the more difficult measurement conditions there (i.e., greater wind fetch) and working from a boat rather than a stable dock as at the Rhode River.

Determining Habitat Requirements

The success of the optical model at predicting individual diffuse attenuation spectra (Figs. 4 and 5) and general relationships between diffuse attenuation coefficients and water-quality parameters (Figs. 7 and 8) suggests that it should be useful for investigating a wide range of conditions not necessarily encountered in the limited sampling. Dennison et al. (1993) determined habitat requirements for SAV survival to a depth of 1 m to be total suspended solids TSS $\leq$ 15 mg l^{-1} and [Chl] $\leq$ 15 μg l^{-1}. From regressions of [Turb] against TSS ([Turb]=0.281·TSS + 0.77, r^2 = 0.88, n = 80, Chincoteague Bay and Rhode River pooled data) the requirement TSS $\leq$ 15 mg l^{-1} translates to [Turb] $\leq$ 5 NTU. Using Turbidity = 5 NTU, [Chl] = 15 μg l^{-1}, g_{440} = 0.3 m^{-1}, and μ_0 = 0.89 (typical growing season values), the optical model predicts $K_d(600)$ [$\approx K_d(PAR)$] = 1.52 m^{-1}, similar to the value of $K_d(PAR)$ reported by Dennison et al. (1993) for survival in 1-m mesohaline and polyhaline regions of Chesapeake Bay. A K_d of 1.52 m^{-1} predicts penetration of 22% of near-surface irradiance to 1 m. This combination of water-quality concentrations and light requirement (i.e., 22%) provides a benchmark for evaluating the depth-limit imposed by other combinations of water-quality concentrations.

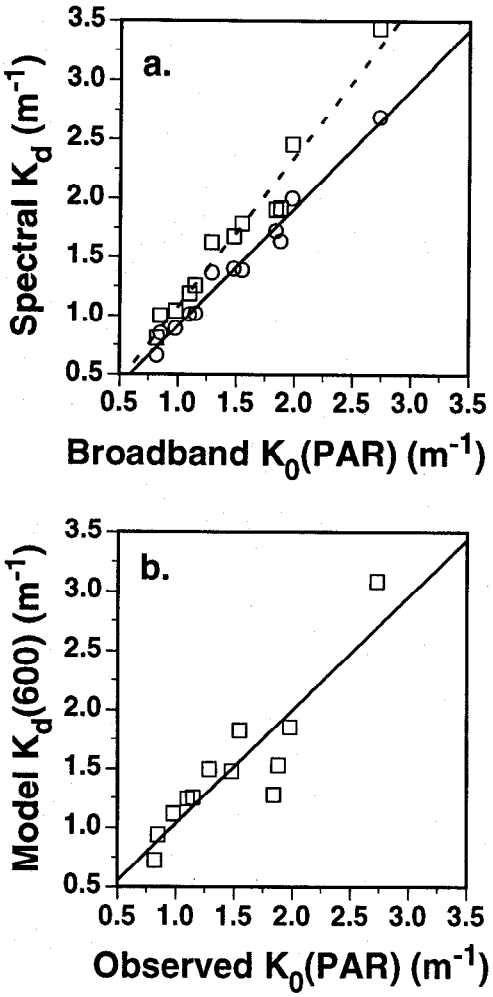

Fig. 6. a. Comparison of diffuse attenuation coefficients (K_d) measured using spectral radiometer with measurements using broadband PAR instrument. -----□-----: calculated using complete spectrum of K_d; ——○——: calculated from single waveband of spectral radiometer centered at 600 nm. b. Comparison of K_d at 600 nm calculated by water quality optical model with measurements using broadband PAR instrument.

To determine the dependence of the 22% penetration-depth on a wider range of water-quality conditions, the parameters [Turb] and [Chl] were varied over a range from 0.1 NTU to 10 NTU and 1 μg l^{-1} to 90 μg l^{-1} respectively, and were used with the optical model to compute contours of constant 22% penetration-depths (i.e., isolumes, Fig. 9). The 1-m isolume passes through the benchmark habitat requirement, ([Chl] = 15, [Turb] = 5) as chosen, but the contours based on predicted $K_0(PAR)$ are surprisingly insensitive to chlorophyll concentration. For example, reduction of [Turb]

TABLE 1. Summary statistics of predicted diffuse attenuation coefficients for 600 nm waveband and for photosynthetically usable radiation (PUR) for different assumed sources of uncertainty in model predictions. Monte Carlo simulations of the optical model were performed by error-corrupting either model coefficients [s_y, σ_{bl}, σ_{400}, s_d, a^*_{ph}, and $b(550)$/turbidity], water quality measurements (g_{440}, [Chl], and [Turb]), or both. Mean value of model coefficients were their estimated values; mean water quality values were g_{440} = 0.3 m^{-1}; [Chl] = 15 $\mu g\ l^{-1}$, and [Turb] = 5 NTU. All error corruptions were done by adding a random normal deviate with zero mean and standard deviation 15% of the mean, except a^*_{ph}, which was multiplied at all wavelengths by a random scalar with a mean of 1 and standard deviation of 0.15. Statistics are based on 500 realizations.

	Source of Error					
	Model Coefficients		Water Quality Measurements		Combined	
Statistic	K_d(600)	K_d(PUR)	K_d(600)	K_d(PUR)	K_d(600)	K_d(PUR)
Mean	1.52	2.04	1.51	2.04	1.51	2.03
Median	1.52	2.04	1.51	2.04	1.51	2.05
Minimum	1.14	1.61	1.04	1.43	0.88	1.30
Maximum	1.92	2.50	2.06	2.66	2.20	2.84
Standard deviation	0.12	0.13	0.16	0.19	0.20	0.23
Coefficient of variation (%)	7.93	6.57	10.7	9.36	13.2	11.5
Skewness	0.13	−0.04	−0.04	−0.04	0.11	0.0
Kurtosis	3.01	2.88	2.89	2.78	2.88	3.03

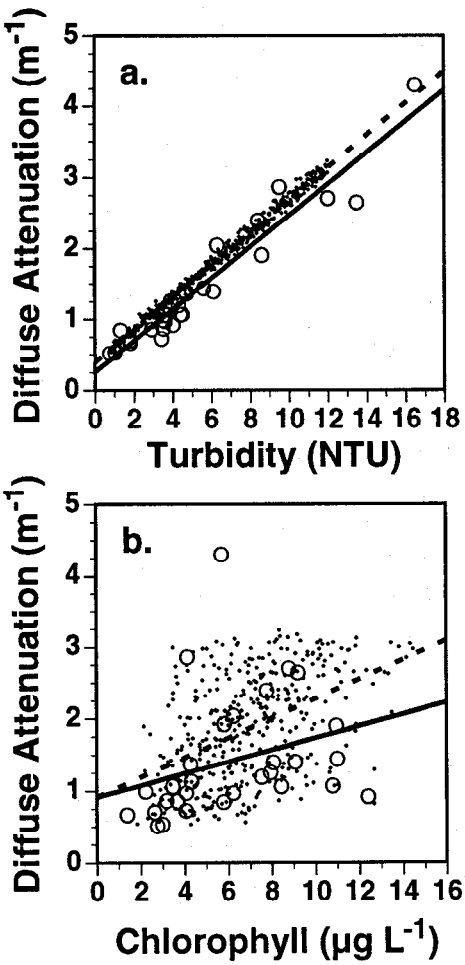

Fig. 7. a. Relationship of diffuse attenuation coefficient at 600 nm to turbidity for Chincoteague Bay, Maryland: (○) measured data; (·) Monte Carlo simulations with optical model. —— regression on measured data; ----- regression on model simulations. b. As (a) but for chlorophyll concentration.

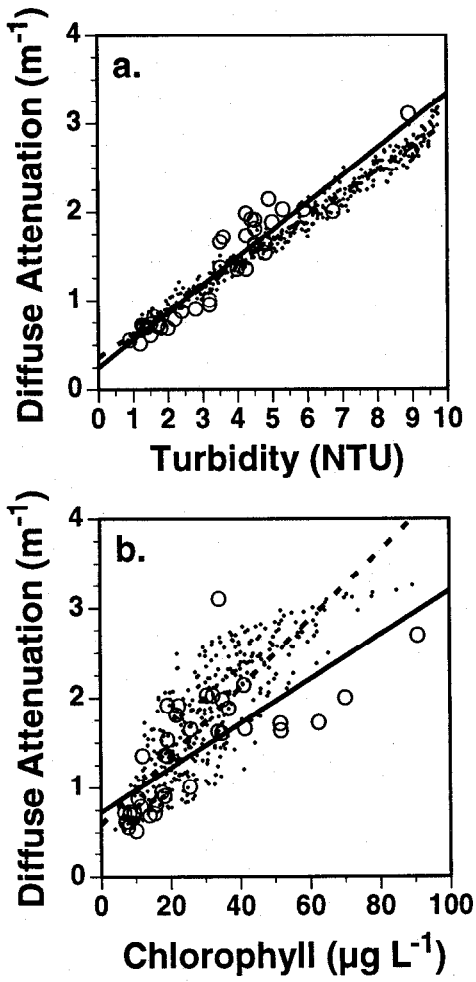

Fig. 8. a. Relationship of diffuse attenuation coefficient at 600 nm to turbidity for the Rhode River, Maryland: (○) measured data; (·) Monte Carlo simulations with optical model. — regression on measured data; ----- regression on model predictions. b. As (a) but for chlorophyll.

TABLE 2. Matrix of simple correlations (r) among water quality variables used in Monte Carlo simulation of the relationship between water quality and $K_d(600)$ predictions by the optical model. A uniform distribution (0.8 to 0.98 for Chincoteague Bay, 0.7 to 0.96 for Rhode River) uncorrelated with any other parameters was used for μ_0. Units: $g_{440}(m^{-1})$; [Chl] ($\mu g\ l^{-1}$); [Turb] (NTU). All correlations significant at $p < 0.01$ except as noted.

Location	Distribution[a]	Simple Correlations [Chl]	Simple Correlations [Turb]
Chincoteague Bay			
g_{440}	U (0.25, 1.06)	0.18[c]	0.32[b]
[Chl]	W (1.6, 6, 2.2)		0.45
[Turb]	U (0.8, 12)		
Rhode River			
g_{440}	N (0.58, 0.25)	0.65	0.67
[Chl]	W (4, 30, 1.8)		0.79
[Turb]	U (0.8, 9.8)		

[a] U = uniform (minimum, maximum); W = Weibull (minimum, scale, shape); N = normal (mean, standard deviation).
[b] Significant at $p < 0.05$.
[c] Not significant.

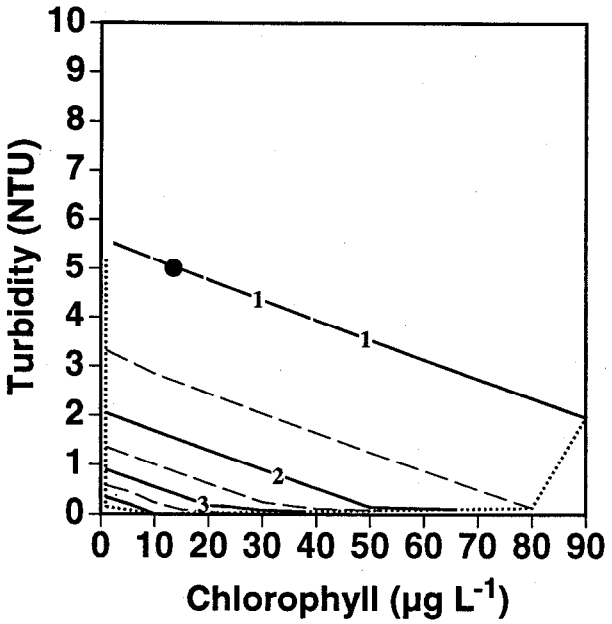

Fig. 9. Contours of depths to which 22 percent of incident quanta in the 585–620 nm waveband [i.e., the best predictor of $K_0(PAR)$] penetrates (i.e., 22 percent isolumes) as a function of phytoplankton chlorophyll and turbidity. K_d (600) calculated by Monte Carlo simulation with the optical water quality model; $g_{440} = 0.3\ m^{-1}$, and $\mu_0 = 0.92$ in all simulations. Circle at (15, 5) is the habitat requirement determined by Dennison et al. (1993) using correspondence analysis in Chesapeake Bay.

from 5 NTU to 4 NTU would permit [Chl] to increase up to 40 $\mu g\ l^{-1}$ without reducing the 22% penetration-depth to less than 1 m. This low sensitivity to [Chl] may be an artifact of the tendency for broadband sensors to measure the attenuation of the most penetrating waveband, which occurs near the absorption minimum of chlorophyll (cf. Fig. 3).

Defining Alternative Survival Criteria

Using the benchmark habitat requirement as a common point defining an acceptable limiting water-quality condition for the 1-m contour, we can use the optical model to explore alternative criteria for defining the habitat requirements of SAV. For ([Chl], [Turb]) = (15,5), the optical model predicts $K_d(600) = 1.52\ (m^{-1})$, $K_d(\widehat{PAR}) = 1.83\ (m^{-1})$, and $K_d(PUR) = 2.04\ (m^{-1})$. For the latter two quantities, the corresponding percentage of surface values at 1 m are 16% of $\widehat{PAR}$ and 13% of PUR. At the benchmark habitat requirement, it is not possible to distinguish which of these quantities determines the depth limits of SAV; but it is an important distinction to make, because the attenuation of PUR and $\widehat{PAR}$ respond differently to changes in water quality. Isolumes based on 16% of $\widehat{PAR}$ and on 13% of PUR are more sensitive to changes in [Chl] than those calculated on the basis of the 600 nm waveband (Fig. 10). For example, to maintain suitable light penetration to 1 m with a 3x increase in [Chl] from 15 $\mu g\ l^{-1}$ to 45 $\mu g\ l^{-1}$ it would be necessary to reduce [Turb] from 5 NTU to 3.9 NTU (i.e., reduction of TSS from 15 $mg\ l^{-1}$ to ca. 11 $mg\ l^{-1}$) based on $K_d(600)$; the same increase in [Chl] would require reduction of [Turb] to 2.65 NTU (reduction of TSS to ca. 6.7 $mg\ l^{-1}$) to maintain penetration of 13% of surface PUR to 1 m (Fig. 10).

Estimating Water-Quality Objectives

In determining water-quality targets for restoring or increasing the depth limits of existing SAV beds, it is useful to plot contours on logarithmic axes, because equidistant changes in either parameter represent equal percentage changes in each variable, independent of units of measurement. Furthermore, remedial action is generally considered in terms of percentage reductions of parameters. Plotting the more conservative depth contours of 13% of PUR as a function of [Chl] and [Turb] (Fig. 11), it is possible to define three regions delimited roughly by the intersection of [Chl] = 10 $\mu g\ l^{-1}$ and [Turb] = 1 NTU. In region I ([Chl] < 10, [Turb] > 1) reducing [Turb] alone would increase depth limits; in region II ([Chl] > 10, [Turb] > 1) both [Chl] and [Turb] must be reduced to increase depth limits; in region III ([Chl] > 10, [Turb] < 1) [Chl] alone dominates the attenuation of PUR (Fig. 11).

The benchmark habitat requirement is close to the border of regions I and II (Fig. 11). It can be

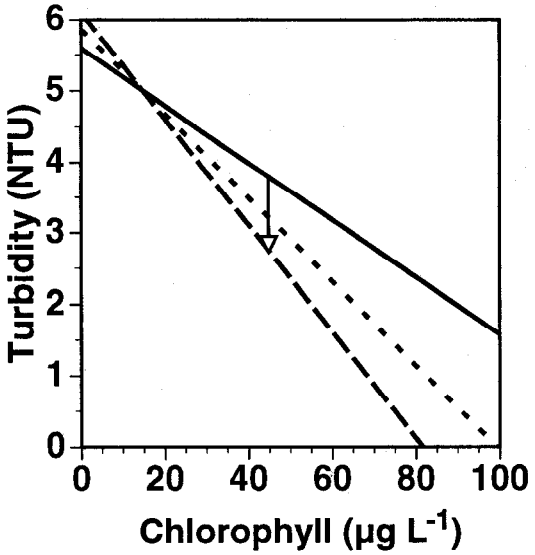

Fig. 10. Contours of water quality parameters producing penetration to 1 m of: —— 22% of most penetrating waveband (i.e., 600 nm); — — 16% of $\widehat{PAR}$ calculated from spectral K_d; and ----- 13% of PUR. Lines intersect at the habitat requirement of [Chl] = 15 µg l^{-1} and [Turb] = 5 NTU determined by Dennison et al. (1993). Arrow indicates reduction in permissible turbidity for three-fold increase in chlorophyll depending on whether PAR or PUR defines the habitat requirement of the plants (see text). Other parameters as in Fig. 9.

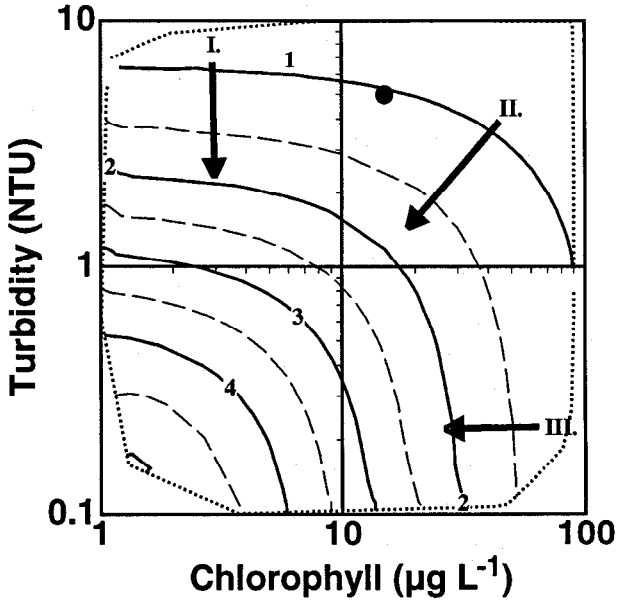

Fig. 11. Depth-contours for penetration of 13% of photosynthetically usable radiation as a function of phytoplankton chlorophyll and turbidity. Axes at [Chl] = 10 µg l^{-1}, [Turb] = 1 NTU divide the plane into regions in which (I) turbidity alone, (II) both turbidity and chlorophyll, or (III) chlorophyll alone must be reduced to increase survival limits for SAV. Circle at [Chl] = 15 µg l^{-1}, [Turb] = 5 NTU is habitat requirement for survival to 1 m determined by Dennison et al. (1993). Other parameters as in Fig. 9.

seen that virtually complete elimination of chlorophyll from that point would not permit SAV survival to 2 m without concomitant reduction of turbidity. The most efficient trajectories (in a mathematical, but not necessarily an economic sense) for increasing depth limits are those perpendicular to the contours. From the benchmark habitat requirement, the closest point on the 2-m isolume is at approximately [Chl] = 10 µg l^{-1}, [Turb] = 1.6 NTU, or approximately 33% reduction in [Chl], and 68% reduction in [Turb].

Discussion

Three water-quality parameters, together with solar zenith angle, were sufficient to model observed spectra of diffuse attenuation (Figs. 4 and 5). The model is constructed in terms of inherent optical properties. Therefore the assumptions of additivity of absorption components (Eq. 5) and linearity with concentration (Eqs. 8a and 9), needed to extrapolate to water-quality conditions not actually encountered, are met. This is not generally true for empirically determined multiple regressions of K_d(PAR) against water-quality parameters. The ability of a single model to predict the spectrum of diffuse attenuation coefficient in two water bodies dominated by different attenuation-producing materials is encouraging. Nevertheless, to use the model for management purposes at other sites requires better understanding of site-specificity of the coefficients in the model. The estimation of specific absorption coefficients and formulation of empirical equations (e.g., Eq. 8b) was done using laboratory measurements of water-quality concentrations and of absorption by dissolved and particulate materials (Figs. 2 and 3). By using measured turbidity to scale scattering coefficients rather than estimating them from K_d(720) (Gallegos et al. 1990), the model is independent of the in situ profiles. Thus, the possibility exists that site-specificity of specific absorption coefficients can be assessed from laboratory measurements of water quality and optical properties.

The water-quality parameters used here are easily measured and, except for perhaps g_{440}, are included in many routine monitoring programs. g_{440} has been correlated with visual color in Pt units (Bowling et al. 1986), with dissolved organic carbon (Gallegos et al. 1990; Cuthbert and del Giorgio 1992 and references therein) and, in fresh water, with tannic acid (Cuthbert and del Giorgio 1992). Chemical measurements add explanatory understanding of factors causing absorption by dissolved matter, but uncertainty in regressions can be expected to reduce precision of model predic-

tions compared with direct optical measurement of g_{440}.

Similarly, the specific-absorption coefficients σ_{bl} and σ_{400} in Eq. 8 would have more physical meaning if formulated in terms of TSS rather than [Turb]; but regressions in Fig. 3 had higher coefficients of determination than similar regressions with TSS as the dependent variable. Wells and Kim (1991) found that the 660-nm absorption and specific scattering coefficients of TSS in the Neuse River (North Carolina, USA) were highly variable. Although nephelometric turbidity is not an inherent optical property, it is an optically based measurement. If turbidity responds similarly to changes in particle size as in situ scattering and absorption, then it is reasonable to expect that turbidity would be a better predictor of the in situ optical properties of suspended particulate matter than mass concentrations.

The benchmark habitat requirement provides a defined light criterion in terms of median diffuse attenuation coefficients and concentrations of optically important water-quality parameters validated against the depth limits of existing SAV beds (Dennison et al. 1993). The habitat requirements developed here extend that of Dennison et al. (1993) by determining the range of water-quality conditions producing the same percentage of light availability at various depths (Fig. 9). It is important to note, however, that the optical model predicts water-column attenuation only. Under high nutrient loading, epiphytes may attenuate an additional 80% of light reaching the surface of the leaves (Twilley et al. 1985). Maintaining nutrient limits (such as those determined by correspondence analysis, Dennison et al. 1993) remains important for limiting growth of epiphytes and for preventing direct adverse physiological effects of elevated nutrients (Burkholder et al. 1992). Figures 9 and 10 should therefore be viewed as providing targets for achieving *minimum* water-quality concentrations for restoration, and for identifying seasonal trends in factors causing degradation of the habitat.

In the future, the optical modeling approach should be useful in further refining the habitat requirements of SAV. For example, the benchmark habitat requirement was determined from growing season medians of water-quality parameters measured at many sites. Does the median light availability determine plant distributions? Is the variance important? Are SAV distributions limited by the duration and timing of extreme attenuation events (e.g., phytoplankton blooms or suspended particle loading/resuspension)? The two factors causing most of the attenuation in many coastal waters, [Chl] and [Turb], are amenable to continuous monitoring, as is PAR and K_d(PAR) (using two vertically offset submersed quantum sensors). Long-term, automated monitoring coupled with optical modeling has the potential to reveal statistical attributes of K_d(PAR) along with the major causes of attenuation required for SAV survival.

The benchmark habitat requirement was associated with an attenuation coefficient for PAR of 1.5 m^{-1}, or 22% of surface PAR (Dennison et al. 1993). For the same water-quality parameters and depth interval, the optical model predicted penetration of 13% of PUR. The depth-contours in Fig. 11 are based on the penetration of 13% of PUR because that criterion produces more conservative limits for chlorophyll (Fig. 10); but how important is the spectral distribution relative to total quanta? Chambers and Prepas (1988) hypothesized that light quality as well as quantity controlled the maximum depth of angiosperm colonization in Alberta lakes. However, their analysis did not consider that, for a given K_d(PAR), Secchi depths are greater in highly colored lakes than in lakes with low color or high turbidity (Koenings and Edmundson 1991). Also, their analysis did not consider the in situ light spectrum in relation to the absorption spectrum of plants. Tomasko (1992) demonstrated morphological responses by the subtropical seagrass *Halodule wrightii* to shading by turtle grass that differed from the same degree of shading (in terms of PAR) by neutral density screens. The plants in those experiments were grown at 65% of incident PAR, which is not very close to their depth limits. If the quantum spectral distribution is important at modest degrees of shading, then the question of whether PAR or PUR determines the depth limit needs to be determined definitively. The difference in acceptable water-quality levels is pronounced (Fig. 10). Whatever improvements are made in our understanding of plant requirements in terms of spectral distribution and timing and variance of attenuation, optical modeling will be an effective tool for translating those requirements into water-quality goals.

Acknowledgments

This research was supported by the Estuarine Habitat Program of the Coastal Ocean Program, National Oceanic and Atmospheric Administration. I thank C. Jarriel for assistance with the data collection and analysis of samples in the laboratory.

Literature Cited

Bowling, L. C., M. S. Steane, and P. A. Tyler. 1986. The spectral distribution and attenuation of underwater irradiance in Tasmanian inland waters. *Freshwater Biology* 16:313–335.

Bricaud, A., A. Morel, and L. Prieur. 1981. Absorption by dissolved organic matter of the sea (yellow substance) in the UV and visible domains. *Limnology and Oceanography* 26:43–53.

Burkholder, J. M., K. M. Mason, and H. B. Glashow, Jr. 1992. Water-column nitrate enrichment promotes decline of eel-

grass, *Zostera marina*: Evidence from seasonal mesocosm experiments. *Marine Ecology Progress Series* 81:163–178.

CHAMBERS, P. A. AND E. E. PREPAS. 1988. Underwater spectral attenuation and its effect on the maximum depth of angiosperm colonization. *Canadian Journal of Fisheries and Aquatic Sciences* 45:1010–1017.

CORRELL, D. L. AND T. L. WU. 1982. Atrazine toxicity to submerged vascular plants in simulated estuarine microcosms. *Aquatic Botany* 14:151–158.

CUTHBERT, I. D. AND P. DEL GIORGIO. 1992. Toward a standard method of measuring color in freshwater. *Limnology and Oceanography* 37:1319–1326.

DENNISON, W. C. 1987. Effects of light on seagrass photosynthesis, growth, and depth distribution. *Aquatic Botany* 27:15–26.

DENNISON, W. C., R. J. ORTH, K. A. MOORE, J. C. STEVENSON, V. CARTER, S. KOLLAR, P. W. BERGSTROM, AND R. A. BATIUK. 1993. Assessing water quality with submersed aquatic vegetation. *BioScience* 43:86–94.

DUARTE, C. M. 1991. Seagrass depth limits. *Aquatic Botany* 40: 363–377.

GALLEGOS, C. L., D. L. CORRELL, AND J. W. PIERCE. 1990. Modeling spectral diffuse attenuation, absorption, and scattering coefficients in a turbid estuary. *Limnology and Oceanography* 35: 1486–1502.

GIESEN, W. B. J. T., M. M. VAN KATWIJK, AND C. DEN HARTOG. 1990. Eelgrass condition and turbidity in the Dutch Wadden Sea. *Aquatic Botany* 37:71–85.

GORDON, H. R. 1991. Absorption and scattering estimates from irradiance measurements: Monte Carlo simulations. *Limnology and Oceanography* 36:769–776.

KIRK, J. T. O. 1981. Monte Carlo study of the nature of the underwater light field in and the relationships between optical properties of turbid, yellow waters. *Australian Journal of Marine and Freshwater Research* 32:517–532.

KIRK, J. T. O. 1984. Dependence of relationship between inherent and apparent optical properties of water on solar altitude. *Limnology and Oceanography* 29:350–356.

KIRK, J. T. O. 1991. Volume scattering function, average cosines, and the underwater light field. *Limnology and Oceanography* 36:455–467.

KOENINGS, J. P. AND J. A. EDMUNDSON. 1991. Secchi disk and photometer estimates of light regimes in Alaskan lakes: Effects of yellow color and turbidity. *Limnology and Oceanography* 36:91–105.

MASKE, H. AND H. HAARDT. 1987. Quantitative in vivo absorption spectra of phytoplankton: Detrital absorption and comparison with fluorescence excitation spectra. *Limnology and Oceanography* 32:620–633.

MCPHERSON, B. F. AND R. L. MILLER. 1987. The vertical attenuation of light in Charlotte Harbor, a shallow, subtropical estuary, southwestern Florida. *Estuarine, Coastal and Shelf Science* 25:721–737.

MOREL, A. 1978. Available, usable, and stored radiant energy in relation to marine photosynthesis. *Deep-Sea Research* 25:673–688.

MOREL, A. AND R. C. SMITH. 1982. Terminology and units in optical oceanography. *Marine Geodesy* 5:335–349.

MOREL, A. AND B. GENTILI. 1991. Diffuse reflectance of oceanic waters: Its dependence on sun angle as influenced by the molecular scattering contribution. *Applied Optics* 30:4427–4438.

ORTH, R. J. AND K. A. MOORE. 1983. Chesapeake Bay: An unprecedented decline in submerged aquatic vegetation. *Science* 222:51–53.

PHILLIPS, D. M. AND J. T. O. KIRK. 1984. Study of the spectral variation of absorption and scattering in some Australian coastal waters. *Australian Journal of Marine and Freshwater Research* 35:635–644.

PIERCE, J. W., D. L. CORRELL, M. A. FAUST, B. GOLDBERG, AND W. H. KLEIN. 1986. Response of underwater light transmittance in the Rhode River estuary to changes in water-quality parameters. *Estuaries* 9:169–178.

PRIEUR, L. AND S. SATHYENDRANATH. 1981. An optical classification of coastal and oceanic waters based on the specific spectral absorption curves of phytoplankton pigments, dissolved organic matter, and other particulate materials. *Limnology and Oceanography* 26:671–689.

ROESSLER, C. S., M. J. PERRY, AND K. L. CARDER. 1989. Modeling in situ phytoplankton absorption from total absorption spectra in productive inland marine waters. *Limnology and Oceanography* 34:1510–1523.

SHORT, F. T. 1991. Light limitation on seagrass growth, p. 38–41. *In* W. J. Kenworthy and D. E. Haunert (eds.), The Light Requirements of Seagrasses: Proceedings of a Workshop to Examine the Capability of Water Quality Criteria, Standards and Monitoring Programs to Protect Seagrasses. National Oceanic and Atmospheric Technical Memorandum, NMFS-SEFC-287. Beaufort, North Carolina.

SHORT, F. T., B. W. IBELINGS, AND C. DEN HARTOG. 1988. Comparison of a current eelgrass disease to the wasting disease of the 1930's. *Aquatic Botany* 30:295–304.

SMITH, W. O., JR. 1982. The relative importance of chlorophyll, dissolved and particulate material, and seawater to the vertical extinction of light. *Estuarine, Coastal and Shelf Science* 15:459–465.

SMITH, R. C. AND K. S. BAKER. 1981. Optical properties of the clearest natural waters (200–800 nm). *Applied Optics* 20:177–184.

THAYER, G. W., D. A. WOLFE, AND R. B. WILLIAMS. 1975. The impact of man on seagrass systems. *American Scientist* 63:288–296.

TOMASKO, D. A. 1992. Variation in growth form of shoal grass (*Halodule wrightii*) due to changes in the spectral composition of light below a canopy of turtle grass (*Thalassia testudinum*). *Estuaries* 15:214–217.

TWILLEY, R. R., W. M. KEMP, K. W. STAVER, J. C. STEVENSON, AND W. R. BOYNTON. 1985. Nutrient enrichment of estuarine submersed vascular plant communities. 1. Algal growth and effects on production of plants and associated communities. *Marine Ecology Progress Series* 23:179–191.

VANT, W. N. 1990. Causes of light attenuation in nine New Zealand estuaries. *Estuarine, Coastal and Shelf Science* 31:125–137.

WEAST, R. C. (ED.). 1980. Handbook of Chemistry and Physics. Chemical Rubber Co., Cleveland, Ohio.

WEIDEMANN, A. D. AND T. T. BANNISTER. 1986. Absorption and scattering coefficients in Irondequoit Bay. *Limnology and Oceanography* 31:567–583.

WELLS, J. T. AND S.-Y. KIM. 1991. The relationship between beam transmission and concentration of suspended particulate material in the Neuse River estuary, North Carolina. *Estuaries* 14:395–403.

WITTE, W. G., C. H. WHITLOCK, R. C. HARRISS, J. W. USRY, L. R. POOLE, W. M. HOUGHTON, W. D. MORRIS, AND E. A. GURGANUS. 1982. Influence of dissolved organic materials on turbid water optical properties and remote-sensing reflectance. *Journal of Geophysical Research* 87:441–446.

Received for consideration, May 5, 1993
Accepted for publication, August 26, 1993